Chapter 3

Digital Atlas of the Rhesus Monkey Brain in Stereotactic Coordinates

M. Mallar Chakravarty*, Stephen Frey, D. Louis Collins

McConnell Brain Imaging Centre,
Montreal Neurological Institute, McGill University
3801 University Street, Montreal, Canada H3A 2B4

*Corresponding author at the following email address:

e-mail: mallar@bic.mni.mcgill.ca

INTRODUCTION

Advances made in the development of stereotaxic spaces have greatly benefited human neuroimaging studies. These coordinate systems allow for the comparison of functional data between subjects, groups, as well as across, scientific laboratories. The original human stereotaxic space was defined by Talairach and Tournoux (1988) using cortical and subcortical landmarks to develop a coordinate system within the human brain and this is currently one of the most widely used human stereotaxic atlases amongst neuroimaging scientists. Since the definition of this initial stereotaxic space, others have been defined using the average of anatomical magnetic resonance imaging volumes (Evans et al., 1993). Using the concept of a common stereotaxic space, multiple techniques have been presented for the automated segmentation of structural magnetic resonance imaging (MRI) data using fully segmented models (Collins et al., 1995; Baillard et al., 2001) or digital atlases (Kikinis et al., 1996; Chakravarty et al., 2006a; Yelnik et al., 2007) which can be customized to a specific subject's individual anatomy.

Researchers rely on the organization and workings of the macaque monkey brain to further understand human brain function, and it is for this reason that MRI scanning is becoming an essential component for scientists using monkeys in their research. Monkey imaging data collected in longitudinal (Malkova et al., 2006), functional (Logothetis et al., 1999; Vanduffel et al., 2001; Tolias et al., 2005), lesion (Petrides, 2000; Izquierdo et al., 2004), anatomical track tracing (Petrides and Pandya, 2006), cannulae localization (Frey et al., 2004), *ex vivo* (Malandain et al., 2004; Annese et al., 2006; Dauguet et al., 2007) and population (Makris et al., 2007) studies would benefit from the translation of these techniques. Thus, it is now imperative, with the increasing number of macaque monkey studies emerging, that a standardized anatomical space and coordinate system be set in place to aid in the localization and targeting of brain areas and structures. This would afford the community the opportunity to compare coordinate locations of their findings, as is typically done in the human literature.

In this chapter we develop three concepts: the first is the creation of a 3D digital atlas using modified contour data presented in the present atlas. Since these contours are derived from a set of serial histological data, several slice-to-slice nonlinear inconsistencies are present. As in the acquisition of any histological dataset, if the slices acquired were merely stacked, the resulting volume would be inhomogeneous with respect to the slice-to-slice morphology. Thus, image processing and reconstruction techniques must be used in order to minimize these inconsistencies. The second concept is the implementation of a coordinate system we call the MNI monkey space. This space is derived from the unbiased nonlinear average of MRIs acquired from seven rhesus macaque monkey brains and is part of a common stereotaxic coordinate system developed for non-human rhesus primates (Macaca mulatta) and cynomulgus primates (Macaca fascicularis) at the Montreal Neurological Institute (Frey, Pandya, Chakravarty, Petrides, and Collins, unpublished studies; see www.bic.mni.mcgill.ca/atlases). The final concept is the warping of the reconstructed contour atlas to effectively fit the nonlinear MRI average. This final step allows for a simple transformation between the MNI rhesus monkey space and the plates and coordinates of the current atlas, enabling the identification of structures in individual animals while at the same time permitting the comparison of findings across different imaging and basic scientific studies. Computer software is provided on the DVD of the present atlas enabling individual monkey MRI volumes to be placed into the coordinate space of this atlas. This software is also provided on the web at http://www.bic.mni.mcgill.ca/atlases/MNI_Rhesus.

METHODS

The slice-to-slice morphological correction techniques are based on work that was created for the reconstruction of a set of serial histological data of the basal ganglia and the thalamus in the human (Chakravarty et al., 2006a). One of the goals of the original work was to develop a method for the reconstruction of data lacking imaging references. These techniques were adapted for the monkey dataset so that the high quality segmentations from the original atlas could be exploited.

CORONAL SLICES OF THE ATLAS

The contours reconstructed to create this atlas were taken from the scalable vector graphic images (SVG) files described in the present chapter by Kötter and colleagues on the CoCoMac Paxinos 3D Tool (see Fig 1). These Figures were converted to grey-level 2D minc images (the standard file format used at the MNI), for image processing purposes.

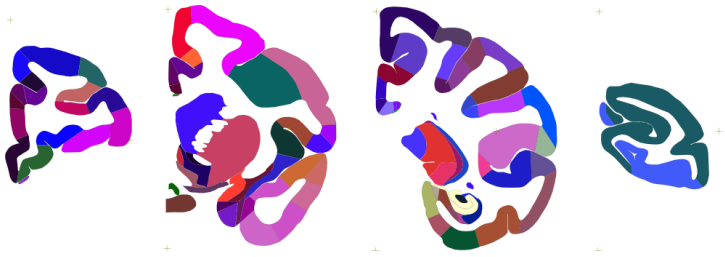

Figure 1. Examples of the input data. Original input data used as depicted in the CoCoMac application. Shown here (from left to right) are figures 14, 44, 84, and 144.

NONLINEAR REGISTRATION AND REGISTRATION WITH ANATOMICAL CONSTRAINTS

Based on our original work (Chakravarty et al., 2006a), a 2D nonlinear transformation was estimated at each slice using the ANIMAL algorithm (Collins et al., 1995; Collins and Evans, 1997). ANIMAL is an iterative algorithm which estimates a 2D deformation field on a lattice of nodes to match a source slice or volume to a target slice or volume. The nonlinear transformation is estimated in a hierarchical fashion, where large deformations are estimated on slices blurred with a Gaussian kernel with a large full-width at half maximum (FWHM). The transformation estimated at a lower resolution is used as the input for the next step, where it is refined by estimating a transformation on slices which have been blurred with a Gaussian kernel with a smaller FWHM. This procedure is repeated (typically between 2–4 times), and is known as the outer loop. At each step of the outer loop, the ANIMAL algorithm is applied iteratively in an inner loop to optimize the nonlinear transformation that maximizes the similarity between a source slice or volume and a target slice or volume. The transformation estimation consists of two steps: the first is the estimation of a translation at each node which maximizes the local similarity measure; the second is a smoothing step to ensure that a continuous deformation field has been estimated. This is how ANIMAL is typically used to align MRI volumes using intensity and contrast information (e.g., in the context of intra-modality MRI-to-MRI or histology-to-histology matching), and ANIMAL was used in this fashion for MRI-template creation through the average of numerous MRIs (Evans et al., 1993), as well as atlas-to-template warping (Chakravarty et al., 2006a,b).

However, the input contour data contains valuable anatomical information that can be exploited to further refine the slice-to-slice anatomical consistency. Inspired by the work in Collins et al. (1998) an additional optimization of the nonlinear transformation was performed using the contour information at each slice. In the original work, additional optimizations were performed by minimizing the chamfer distance (Borgefors, 1984), an approximation of the more accurate Euclidean distance (Duda et al., 2000), between segmentations of cortical sulci. The implementation used in the present work refined the optimization procedure by using two different distance maps. The first map estimated the distance from each voxel in the background to the edge of the foreground (i.e., to the edge of the structures defined in the atlas). The second map estimated the distance from each voxel in the foreground to the closest edge of a structure defined in the atlas.

SLICE-TO-SLICE MORPHOLOGICAL CORRECTION TECHNIQUES

Since the segmentations used in this atlas were derived from serial histological data, the slice-to-slice variation in morphology must be accounted for. This type of morphological variation is well described with the reconstruction of *ex vivo* data (Malandain, 2004; Chakravarty et al., 2006a; Dauguet et al., 2007). The parameters for slice-to-slice registration used for this dataset were taken from Chakravarty et al., (2006a).

Global volumetric morphological consistency was achieved by enforcing local slice-to-slice morphological consistency. The non-linear registration technique described in the previous section was used to estimate six 2D nonlinear transformations for each slice. The first three transformations matched intensity data and minimized the chamfer distance error between distance maps for slice *i* and each of the slices which came before it *(slices i–1, i–2,* and *i–3*) in the series. Three additional transformations were estimated in the same fashion between *slice i* and the 3 slices which came after it in the series (*slices i+1, i+2,* and *i+3*). These transformations were averaged and then applied to the contours of *slice i*. Thus, global slice-to-slice consistency was enforced by achieving local slice-to-slice consistency (Fig. 2).

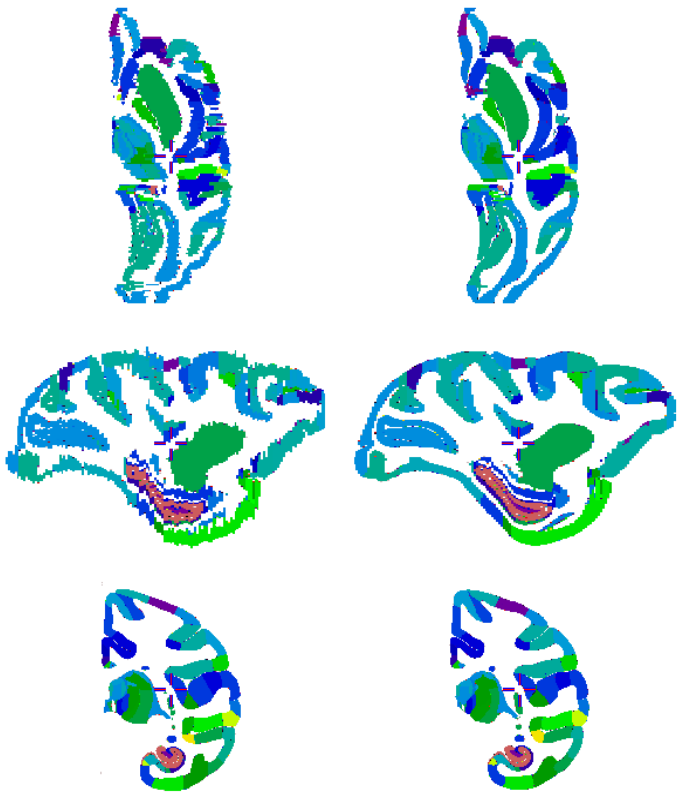

Figure 2. Results of the slice-to-slice realignment. From left to right: Original data stacked to create an image volume, and the slices of this image volume morphologically corrected to create homogeneous representations of the anatomy. From top to bottom: Reconstructed axial and sagittal views and an original coronal slice.

MRI ATLAS TEMPLATE

Since the reconstructed atlas developed above had no reference data (such as MRI or block-face images), it was matched to an average MRI template derived from the average of 7 rhesus monkeys (Macaca mulatta, 2 females, 5 males, approx., 3.3 to 13.1 kg at the time of MRI). The protocols used were approved by the Montreal Neurological Institute Animal Ethics Committee and conformed to the Canadian Council of Animal Care guidelines for the humane care of laboratory animals.

MRI data was acquired on a Siemens Sonata 1.5T magnet in the context of stereotaxic surgery planning with a 3D transverse T1w acquisition (TE=9.5ms, TR=22ms). Each monkey was initially tranquilized with Ketamine (10 mg/kg, Ketaset) and acepromazine (0.4 mg/kg, im, Atravet), and deep anesthesia was maintained with isoflurane (3–4% at induction and 0.8–2%, Isoflo) throughout the procedure. The monkey was then placed in the magnet in the standard supine position. Throughout the scan, the monkeys oxygen saturation levels (SPO_2) and heart rate were monitored using pulse oximetry with an infrared sensor that was clipped to the animals hallux through a fiber optic cable that was attached to a monitor. Data was acquired with different voxel sizes as the sequence was optimized over time, varying from 0.305mm^3 to 0.125mm^3.

Image pre-processing included non-uniform intensity correction (Sled et al., 1998) and intensity normalization to a range of 0–100. One monkey was chosen to serve as the initial target (T0). Registration of the remaining 6 animals was initialized using manually identified homologous landmarks that included the center of the left and right eyeballs, the anterior commissure (AC), the posterior apex of the 4th ventricle as seen in a midline sagittal image, the most anterior aspect of the genu and the most posterior aspect of the corpus callosum, and the intersection of the central sulcus with the longitudinal fissure. All the monkeys were registered with a 7 parameter transformation (3 rotations, 3 translations, 1 scale), resampled and averaged in the space of T0 to form the initial average (A0).

The center of the AC and posterior commissure (PC) were identified on A0 and used to define a transformation to bring the center of the AC to the origin (0,0,0), align the PC along the negative y-axis, and align the longitudinal fissure in the x=0 plane. A0 was resampled onto a 0.25mm isotropic grid to form the first target volume Alin0.

After this initialization, the automatic cross-correlation based registration program minctracc (Collins et al., 1994) was used to compute the optimal 9-parameter transformation (3 translations, 3 rotations, 3 scales) that mapped each monkey to Alin0. Each MRI volume was resampled with the recovered transformations and averaged together to form Alin9. This process was repeated, estimating a 12-parameter transformation (3 translations, 3 rotations, 3 scales, 3 skews) to form Alin12. Afterwards, non-linear registration was used to refine the average. The ANIMAL program (Collins et al., 1995) was used to estimate the non-linear deformation field that best aligned local neighborhoods between each monkey volume and the average target. The non-linear registration began by estimating a grid with 3mm spacing. All MRI volumes were resampled through the recovered non-linear transformation to form Anl3. This process was repeated twice, using a grid spacing of 2mm with the Anl3 target to form the Anl2 target, and then using a grid spacing of 1mm to form the Anl1 target. At this point, deformation fields were estimated to map all monkeys into the same space. The resulting volume can be seen in the rightmost column of Fig 3 and in Fig 4.

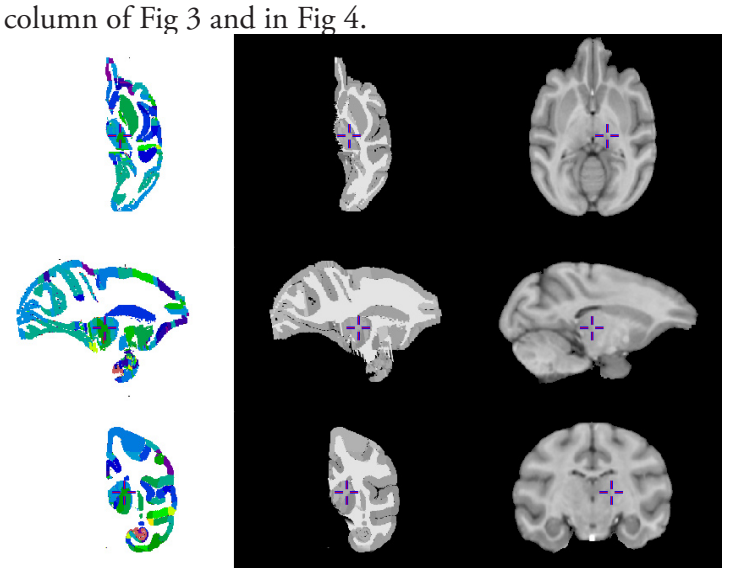

Figure 3. Pseudo-MRI creation. From left to right: Reconstructed contour atlas, pseudo-MRI created by modifying the intensities of the reconstructed contour atlas, and MRI atlas template derived from the average of 7 rhesus monkeys. From top to bottom: Axial, sagittal, and coronal slices.

LINEAR ATLAS-TO-TEMPLATE WARPING

To establish a voxel wise correspondence between the reconstructed atlas and the MRI-template, the atlas was first aligned with the MRI template using 24 homologous landmark pairs defined on both the reconstructed atlas and the MRI template. These landmark pairs were used to define a 12-parameter transformation to bring the atlas into coarse alignment with the MRI template. While this initial transformation brings these two volumes into alignment, the quality of the alignment is fairly coarse and it cannot account for nonlinear morphological differences between the reconstructed atlas and the MRI-template as seen by comparing columns 2 and 3 in Fig 3 or the middle column of Fig 4.

NONLINEAR ATLAS-TO-TEMPLATE WARPING

To account for these morphological differences, we used the ANIMAL algorithm once more to estimate a nonlinear transformation to match the reconstructed atlas to the template. Since ANIMAL depends on the contrast between the two image volumes to be similar for corresponding structures, the reconstructed atlas required modification prior to the estimation of a nonlinear atlas-to-template transformation. Thus the intensities assigned to each structure were modified to approximate those of the MRI target volume. We call this modified volume a pseudo-MRI (Chakravarty et al., 2006a, b; see middle column in Fig 3).

The 12-parameter transformation was used as the input for the nonlinear transformation estimation process. Using the pseudo-MRI, a transformation can be estimated to match the reconstructed atlas volume directly to the MRI volume. An exclusion mask was first created so that the cerebellum, the brainstem, and the left hemisphere of the MRI-template were eliminated from the transformation estimation process. The nonlinear registration was initiated by estimating a transformation on a grid with 6mm spacing. This process was repeated three more times by estimating transformations on grids of 3, 2, and 1 mm, where the transformations estimated at coarser resolutions were used as the input to the next step.

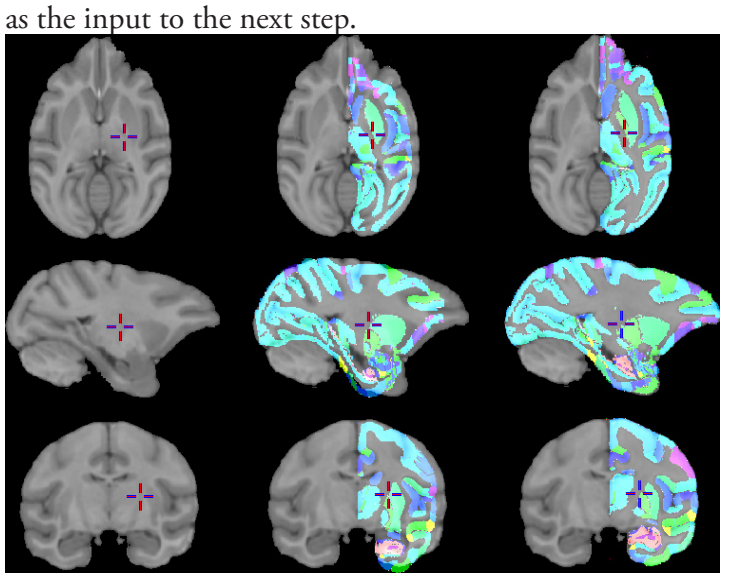

Figure 4. Atlas to template warping. From left to right: MRI template derived from the average of 7 rhesus monkeys; atlas warped to the MRI template using a 12-parameter linear transformation; atlas warped to the template by refining the initial fit using a nonlinear transformation. From top to bottom: Axial, sagittal, and coronal slices.

RESULTS

SLICE REALIGNMENT RESULTS

The results from the slice-to-slice morphological correction are shown in Fig 2. The figure shows the original data stacked to create an image volume of contours on the right, whereas on the left of the image, the realigned data is presented. Since each structure is identified using a unique intensity to label the structure, improved slice-to-slice alignment allows for enhanced structure visualization (as is demonstrated on the right of Fig 2).

ATLAS-TO-TEMPLATE WARPING

To properly visualize the atlas with an MRI volume, warping onto an MRI template was required using the pseudo-MRI created to enable a direct estimation of the atlas-to-template transformation used in Fig 3. On the left of Fig 3, the digital contour based atlas is shown after slice-to-slice realignment, in the middle the modified contour based atlas is used to create a pseudo-MRI, and on the right the atlas template is shown. The results demonstrate how the contour atlas was effectively modified to simulate the intensities and contrast of the MRI-template.

The results of the subsequent atlas-to-template nonlinear warping are shown in Fig 4. The left column of the image shows the MRI-template, the middle column demonstrates the atlas-to-template alignment subsequent to linear transformation, and the right column demonstrates improved alignment by nonlinear warping. Significant improvement in structural alignment can be observed in both cortical and subcortical structures.

SUMMARY

In this chapter we describe techniques used for the reconstruction of the present print rhesus monkey brain atlas and the creation of a digital 3D average atlas that can be used to transform between the MNI rhesus monkey space and the plates of this atlas. Using contours defined in the CocoMac application, a nonlinear transformation was estimated for each slice to correct slice-to-slice anatomical inconsistencies. The reconstructed contour atlas was nonlinearly warped to fit an atlas template derived from the nonlinear average of seven rhesus monkeys in order to define the MNI rhesus monkey space. The user is capable of transforming coordinates to and from MNI rhesus monkey space to the coordinates defined in the present atlas using the simple linear transformations that are included in this chapter and on the DVD.

ACKNOWLEDGMENTS

The manual drawings of the coronal sections from the *Rhesus Monkey Atlas in Sterotactic Coordinates* were made and provided by Christoph Edel, Gleb Bezgin, and Rolf Kötter from the Department of Cognitive Neuroscience, Radbound Nijmegen Medical Center, the Netherlands.

APPENDIX: PRINT ATLAS-TO-MRI AND MRI-TO-PRINT ATLAS COORDINATE TRANSFORMATIONS

There are two methods to map coordinates between the print atlas and the stereotaxic MNI rhesus monkey space coordinate system. The first is a linear transformation and can be computed by hand (or with a simple spreadsheet). The second uses a nonlinear transformation and must use scripts provided on the DVD included with the atlas or the webpage www.bic.mni.mcgill.ca/atlases/MNI_Rhesus. Only the manual technique is described here as the documentation on the DVD and webpage describe the use of the automated scripts.

The first method uses a linear transformation to map coordinates between the atlas and the MNI rhesus monkey space coordinate system. This method is an approximation, since the nonlinear differences between the atlas and the MNI rhesus monkey space MRI template are not accounted for. The mapping errors will be similar to those seen in the middle column of Fig 4.

MAPPING FROM ATLAS TO MRI TEMPLATE

Needed: Figure number F, medial to lateral distance L, and superior/inferior distance S (from left side ruler).

X = (L*0.88138) – (F*0.01556) – (S*0.01450) –1.2849
Y = (L*0.12061) + (F*0.96617) – (S*0.06118) + 4.2790
Z = – (L*0.01916) – (F*0.03193) + (S*0.96358) –16.5076

Where X, Y and Z are in mm in the MNI rhesus monkey space coordinate system. Where the center of the anterior commissure (AC) was selected as the origin of the coordinate system (x = 0, y = 0, z = 0). Positive y-coordinates increase in the rostral direction while negative y-coordinates decrease in the caudal direction from AC. Positive x-coordinates increase towards the right (and decrease towards the left). Z-coordinates increase superiorly and decrease inferiorly.

MAPPING FROM MRI TEMPLATE TO ATLAS

Needed: X, Y, Z (as defined above) in the stereotaxic MNI rhesus monkey space coordinate system.

L = (X*1.13240) + (Y*0.01884) + (Z*0.01824) + 1.67555
F = – (X*0.14023) + (Y*1.03486) + (Z*0.06359) – 3.55865
S = (X*0.01787) + (Y*0.03466) + (Z*1.04026) + 17.04690

REFERENCES

Annese, J., Sforza, D.M., Dubach, M., Bowden, D. and Toga, A.W. (2006). Postmortem high- resolution 3-dimensional imaging of the primate brain: Blockface imaging of perfusion stained tissue. *NeuroImage*. 30, 61–69.

Baillard, C., Hellier, P. and Barillot, C. (2001). Segmentation of brain 3D MR images using level sets and dense registration. *Med Image Anal*. 5, 185–194.

Borgefors, G. (1984). Distance Transformations in Arbitrary Dimensions. CVGIP. 27, 321–345.

Chakravarty, M.M., Bertrand, G., Hodge, C.P., Sadikot, A.F. and Collins, D.L. (2006a). The creation of a brain atlas for image guided neurosurgery using serial histological data. *NeuroImage*. 30, 359–376.

Chakravarty, M.M., Sadikot, A.F., Mongia, S., Bertrand, G. and Collins, D.L. (2006b). Towards a multimodal atlas for neurosurgical planning. In *Ninth International Conference on Medical Image Computing and Computer Assisted Intervention MICCAI 2006*, volume 2 of LNCS, pages 389–396, Copenhagen, Denmark. Springer.

Collins, D.L. and Evans, A.C. (1997). ANIMAL: Validation and application of non-linear registration based segmentation. *IJPRAI*. 11, 1271–1294.

Collins, D.L., Holmes, C.J., Peters, T.M. and Evans, A.C. (1995). Automatic 3D Model Based Neuroanatomical Segmentation. *Hum Brain Map*. 3, 190–208.

Collins, D.L., Le Goualher, G. and Evans, A.C. (1998). Non-linear cerebral registration with sulcal constraints. In *First International Conference on Medical Image Computing and Computer-Assisted Intervention MICCAI 1998*, LNCS, pages 974-84, Cambridge, MA, USA, October 1998.

Collins, D.L., Neelin, P., Peters, T.M. and Evans, A.C. (1994). Automatic 3D Intersubject Registration of MR Volumetric Data in Standardized Talairach Space. *J Comput Ass Tom*. 18,192–205.

Dauguet, J., Delzescaux, T., Condé, F., Mangin, J-F., Ayache, N., Hantraye, P. and Frouin, V. (2007). Three-dimensional reconstruction of stained histological slices and 3D non-linear registration with *in vivo* MRI for whole baboon brain. *J Neurosc Meth*. 164, 191–204.

Duda, R.O., Hart, P.E. and Stork, G. (2000). *Pattern Classification* (2nd edition). John Wiley & Sons, Inc., New York, USA.

Evans, A.C., Collins, D.L., Mills, S.R., Brown, E.D., Kelly, R.L. and Peters, T.M. (1993). 3D statistical neuroanatomical models from 305 MRI volumes. *In IEEE Nuclear Science Symposium and Medical Imaging Conference*, pages 1813–1817, San Francisco, USA.

Frey, S., Comeau, R., Hynes, B., Mackey, S. and Petrides, M. (2004). Frameless stereotaxy in the nonhuman primate. *NeuroImage*. 23, 1226–1234.

Izquierdo, A., Suda, R.K. and Murray, E.A. (2004). Bilateral orbital prefrontal cortex lesions in rhesus monkeys disrupt choices guided by both reward value and reward contingency. *J. Neurosci*. 24, 7540–7548.

Kikinis, R., Shenton, M.E., Iosifescu, D.V., McCarley, R.W., Saiviroonporn, P., Hokama, H.H., Robatino, A., Metcalf, D.,Wible, C.G., Portas, C.M., Donnino, R.M. and Jolesz, F.A. (1996). A Digital Brain Atlas for Surgical Planning, Model-Driven Segmentation, and Teaching. *IEEE TVCP*. 2, 232–241.

Logothetis, N., Guggenberger, H. Peled, S. and Pauls, J. (1999). Functional imaging of the monkey brain. *Nat. Neurosci*. 2, 555–562.

MacDonald, D. (1998). A Method for Identifying Geometrically Simple Surfaces from Three Dimensional Images. PhD thesis, McGill University.

Makris, N., Papodimitriou, G.M., van der Kouwe, A., Kennedy, D.N., Hodge, S.M., Dale, A.M., Benner, T., Wald, L.L., Wu, O., Tuch, D.S., Caviness, V.S., Moore, T.L., Killiany, R.J., Moss, M.B. and Rosene, D.L. (2007). Frontal connections and cognitive changes in normal aging rhesus monkeys: a DTI study. *Neurobiol Aging*. 28, 1556–1567.

Malandain, G., Bardinet, E., Nelissen, K. and Vanduffel, W. (2004). Fusion of autoradiographs with an MR volume using 2D and 3D linear transformations. *NeuroImage*. 23, 111–127.

Malkova, L., Heuer, E. and Saunders, R.C. (2006). Longitudinal magnetic resonance imaging study

of rhesus monkey brain development. *EJN*. 24, 3204–3212.

Petrides, M. and Pandya, D.N. (2006). Efferent association pathways originating in the caudal prefrontal cortex in the macque monkey. *J. Comp. Neurol*. 498, 227–251.

Sled, J.G., Zijdenbos, A.P. and Evans, A.C. (1998). A Nonparametric Method for Automatic Correction of Intensity Nonuniformity in MRI Data. *IEEE TMI*. 17, 87–97.

Talairach, J. and Tournoux, P. (1998). Co-Planar Stereotaxic Atlas of the Human Brain. Georg Thieme Verlag, Stuttgart, Germany.

Tolias, A.S., Sultan, F., Augath, M., Oeltermann, A., Tehovnik, E.J., Schiller, P.H. and Logothetis, N.K. (2005). Mapping cortical activity elicited with electrical microstimulation using fMRI in the macaque. *Neuron*. 48, 901–911.

Vanduffel, W., Fize, D., Mandeville, J.B., Nelissen, K., Van Hecke, P., Rosen, B.R., Tootell, R.B.H. and Orban, G. (2001). Visual motion processing investigation using contrast agent-enhanced fMRI in awake behaving monkeys. *Neuron*. 32, 565–577.

Yelnik, J., Bardinet, E., Dormont, D., Malandain, G., Ourselin, S., Tandé, D. Karachi, C., Ayache, N., Cornu, P. and Agid, Y. (2007). A three dimensional, histological and deformable atlas of the human basal ganglia. I. atlas construction based on immunohistochemical and MRI data. *NeuroImage*. 34, 618–638.